LEGIBILITY NOTICE

A major purpose of the Technical Information Center is to provide the broadest dissemination possible of information contained in DOE's Research and Development Reports to business, industry, the academic community, and federal, state and local governments.

Although a small portion of this report is not reproducible, it is being made available to expedite the availability of information on the research discussed herein.

-LA-UR -90-705

LA-UR--90-705

DE90 008992

TITLE: **REAL-TIME FOURIER TRANSFORM SPECTROMETRY FOR FLUORESCENCE IMAGING AND FLOW CYTOMETRY**

AUTHOR(S): **Tudor N. Buican**

SUBMITTED TO: **SPIE Proceedings, 1990 (Lasers & Optics in Medicine & Biology)**

Los Alamos National Laboratory
Los Alamos, New Mexico 87545

Real-Time Fourier Transform Spectrometry for Fluorescence Imaging and Flow Cytometry

Tudor N. Buican
Life Sciences Division
Los Alamos National Laboratory, Los Alamos, NM 87545

ABSTRACT

We present a Fourier transform (FT) spectrometer that is suitable for real-time spectral analysis in fluorescence imaging and flow cytometry. The instrument consists of (i) a novel type of interferometer that can be modulated at frequencies of up to 100 kHz and has a high light throughput; and (ii) a dedicated, parallel array processor for the real-time computation of spectral parameters. The data acquisition array processor can be programmed by a host computer to perform any desired linear transform on the interferogram and can thus separate contributions from multiple fluorochromes with overlapping emission spectra. We describe optics configurations for use in both flow cytometry and fluorescence microscopy. The integration of a flow cytometer and a spectral imaging fluorescence microscope is discussed, and the concepts of direct and reversed "virtual sorting" are introduced.

1. INTRODUCTION

The spectral analysis of the fluorescence emitted by cells and cell organelles is fundamental to analysis in both fluorescence flow cytometry and fluorescence microscopy. Indeed, most fluorescence analysis applications require that the total fluorescence emitted by a particle in flow or by a pixel in the microscopy specimen be resolved into contributions from several emission spectra, which can be either the characteristic spectra of several simultaneous fluorochromes, or the modified spectra of a metachromatic fluorochrome. Although conventional systems used in biological applications perform a coarse spectral analysis by dividing the spectrum into a few spectral channels, performing a finer spectral analysis by means of monochromators or polychromators has been attempted, with moderate success, even on flow instruments [1, 2]. We show in this article that Fourier transform spectrometry, which was originally introduced as a solution to the detector noise problem in far infrared spectrometers and is currently being applied to spectral analysis in many spectral regions [3, 4], offers the light throughput, spectral resolution, speed of analysis, and flexibility, required for fluorescence analysis in both flow and imaging instruments

An FT spectrometer consists of an interferometer that encodes the spectral information into an intensity distribution that varies as a function of time or position and a computer that extracts the spectral information from this distribution. Although the use of FT spectrometers in flow or imaging instruments is desirable because of their high light throughput, the speed at which they usually acquire and analyze spectral data makes them unsuitable for such applications. In order to bring the speed of acquisition of multiple spectral parameters to levels compatible with flow cytometric analysis and image acquisition, we approached the speed limitations of FT spectrometers in new ways [5]: (i) we developed a novel interferometer [6] that has no moving parts and can thus be modulated at high frequencies; and (ii) we developed a data acquisition array processor [7] that can process in real time the high-frequency interferograms produced by the interferometer. As will be shown in what follows, the use of real-time digital signal processing is particularly useful in flow and imaging applications in which multiple fluorochromes with overlapping emission spectra are being used and in which the contributions of the individual fluorochromes, rather than the total emission spectra, are of interest. Furthermore, by virtue of the numerical, rather than the optical, spectral analysis they perform, FT flow and imaging instruments can be integrated from the point of view of data analysis and instrument setup. By sharing data and configuration information, integrated FT flow cytometers and fluorescence microscopes can use morphological information in the interpretation of population data ("virtual sorting") and population-level information in the quantitation of morphologies within populations ("reversed virtual sorting").

2. THE BIREFRINGENT INTERFEROMETER

The birefringent interferometer (Fig. 1) consists of a birefringent modulator placed between two polarizers. The polarizers can be either parallel or perpendicular (see below), and the principal axes of the modulator are at 45° relative to the polarizers. This optical system, previously used as an intensity modulator for monochromatic light, can be shown to be an interferometer, the stroke length of which depends on the maximum birefringence attained by the birefringent modulator. A multiple window photoelastic modulator was found to achieve birefringence levels that lead to useful spectral resolution when used in an FT spectrometer.

If l is the thickness of the birefringent modulator and ω is the angular frequency of the incident light, the phase difference, $\Delta\phi$, introduced by the modulator between the x and y components of the electric vector is $\Delta\phi = \omega l/c\ \mu$, where c is the vacuum speed of light, and $\mu = n_x - n_y$. If we define light intensity as $I = < |E|^2 >$, where the angular

brackets denote the time average, then it can be shown that, for optical elements oriented as in Fig. 1, and for unpolarized incident light of intensity I_0, the output intensity is given by $I_{||} = I_0/4\ [1 + \cos(l/c\ \omega\mu)]$. If polarizer P_2 is a polarizing beam splitter, then output intensities corresponding to both parallel and crossed polarizers can be measured simultaneously (see below). As the intensity in the output that corresponds to crossed polarizers is $I_\perp = I_0/4\ [1 - \cos(l/c\ \omega\mu)]$, the difference signal, $I = I_{||} - I_\perp$, which can be obtained by using two detectors and a differential amplifier, is $I = I_0/2 \cos(l/c\ \omega\mu)$. It is this difference signal that will be considered in what follows.

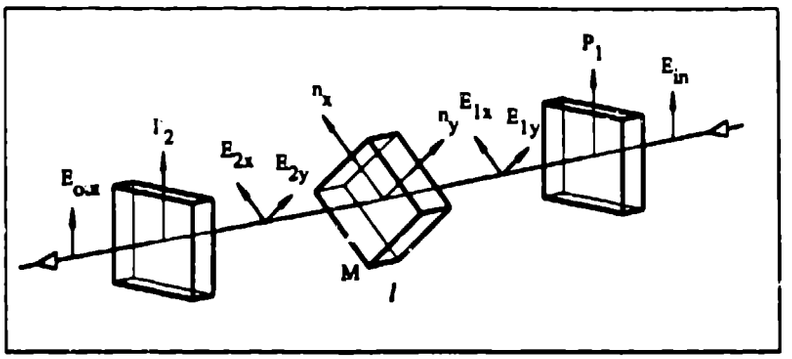

Figure 1. Diagram of the birefringent interferometer. E_{in}, E_{out} - input and output electric vectors; n_x, n_y - refractive indices of the birefringent modulator along its axes x, y; $E_{1x,\ 1y}$, $E_{2x,\ 2y}$ - x, y components of the electric vector at two intermediate locations; M - birefringent modulator; P_1, P_2 - polarizers; l - thickness of the modulator, M.

For polychromatic incident light with intensity spectrum $I_0(\omega)$, the output intensity becomes

$$I(\mu) = 1/2 \int_0^\infty I_0(\omega)\ \cos(l/c\ \omega\mu)\ d\omega \qquad (1a)$$

One can easily see that the output intensity, expressed as a function of μ, is the (cosine) Fourier transform of the intensity spectrum of the incident light, $I_0(\omega)$. The transform in (1a) can be inverted as a cosine transform and this will give

$$I'(\omega) = 4l/\pi c \int_0^m I(\mu) \cos(l/c\ \mu\omega)\ d\mu \qquad (1b)$$

For photoelastic modulators, the birefringence is a harmonic function of time, $\mu = m \sin \omega_0 t$, where ω_0 is the angular frequency at which the modulators are driven, and m is the maximum value of μ. Therefore, the transforms (1a, 1b) can be rewritten as

$$I(t) = 1/2 \int_0^\infty I(\omega) \cos(\gamma\omega \sin \omega_0 t)\ d\omega \qquad (2a)$$

$$I'(\omega) = 8\gamma/T_0 \int_0^{T_0/4} I(t) \cos(\gamma\omega \sin \omega_0 t) \times \times \cos \omega t\ dt \qquad (2b)$$

where $\gamma = lm/c$, and $T_0 = 2\pi/\omega_0$. The response to monochromatic light of frequency ω_1 of an FT spectrometer based on the birefringent interferometer and the transform (2b) can be shown to be

$$I'(\omega) = \gamma/\pi\ [\ \mathrm{sinc}(\gamma(\omega + \omega_1)) + \mathrm{sinc}(\gamma(\omega - \omega_1))\ ] \qquad (3)$$

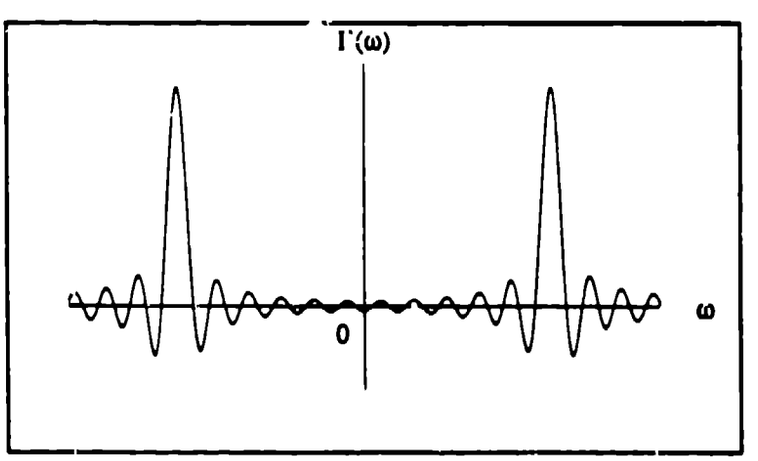

Figure 2. Spectral response function [Eq. (3)] of the FT spectrometer based on a birefringent interferometer and the transform (2b). The two peaks are at $\pm\omega_1$.

which, due to the truncation of the interferogram, gives, essentially, a sinc function spectral response. The spectral response function is shown in Fig.2. Both sinc functions in (3) have a separation between zeros of $\delta\omega = \pi/\gamma$. Thus, independently sampled values of the light-frequency spectrum, $I'(\omega)$, can be obtained by sampling at light frequencies $\omega_n = n\,\pi/\gamma$. The sampling interval, $\delta\omega$, is thus a measure of the spectral resolution of the instrument. If the modulation amplitude is expressed in numbers of "waves", N, at a certain frequency, ω, then the maximum phase difference introduced by the interferometer is $\Delta\phi_{max} = 2\pi N$, which corresponds to a light-frequency sampling interval $\delta\omega = \omega/2N$. Thus, for a modulation amplitude of N waves, the relative spectral resolution at that light frequency is $\delta\omega/\omega = 1/2N$. The minimum interferogram sampling frequency, ω_s, can be defined as twice the maximum frequency component of the interferogram, and is thus given by $\omega_s = 2\gamma\,\omega_0\,\omega_{max}$, where ω_{max} is the highest light frequency. While ensuring that the highest frequencies in the interferogram are properly sampled, uniform sampling at the sampling frequency ω_s results in oversampling of the interferogram toward the end of the stroke of the birefringent interferometer.

Most commercial birefringent modulators are designed to be used for modulating the intensity of monochromatic light. As such, the retardation amplitude they achieve is typically of the order of $\lambda/2$ at some operating light frequency, ω. Under these conditions, the resulting relative spectral resolution is only $\delta\omega/\omega = 1$, which is not useful for spectral analysis. Although photoelastic modulators can be driven to higher retardation amplitudes, useful spectral resolutions can only be achieved by using modulators with multiple windows. An FT spectrometer employing three such windows is shown in Fig.3. The three-window photoelastic modulator, which runs at 85 kHz, was built by Hinds International, Portland, OR. The use of polarizing beam splitter 7 allows a wavelength calibration beam from a low-

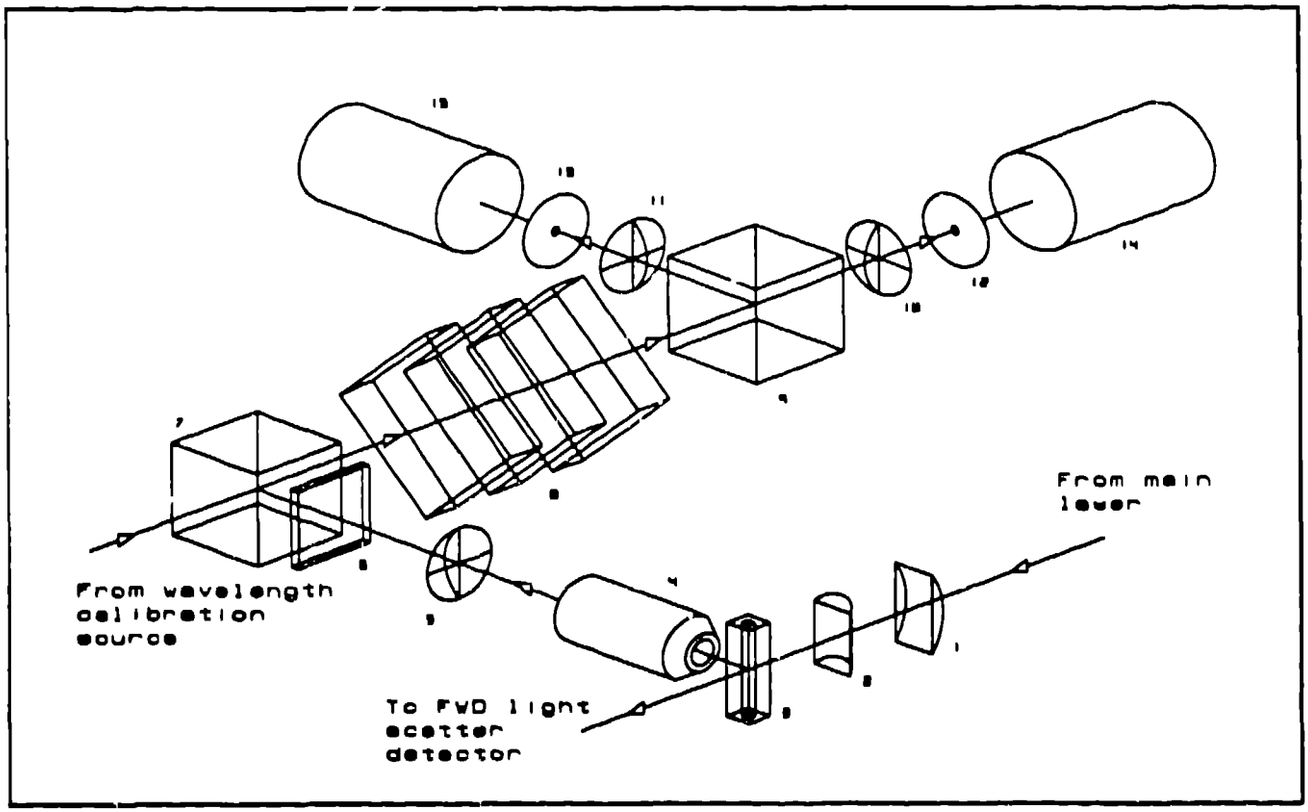

Figure 3. Diagram of a birefringent interferometer for FT spectral analysis in flow cytometry. 1, 2 - cylindrical lenses for focusing the fluorescence excitation laser beam; 3 - flow chamber; 4, 5 - fluorescence collection optics; 6 - long pass optical filter; 7, 9 - polarizing beam splitters; 8 - birefringent modulators; 10, 11 - focusing lenses; 12, 13 - pinholes; 14, 15 - photomultipliers.

power HeNe laser to be introduced into the interferometer. A polarizing beam splitter, 9, in the output of the interferometer allows two signals to be measured. These correspond, respectively, to parallel and crossed orientations of

the interferometer polarizers. As the two signals have ac components of opposite sign while having the same dc component, the difference between the two signals obtained by means of a differential amplifier (not shown in Fig. 3) doubles the amplitude of the interferogram and eliminates the dc component. The difference signal is further processed by digital signal processing electronics discussed in the next section.

3. DIGITAL SIGNAL PROCESSING AND SIGNAL PROCESSING ELECTRONICS

The transform in (2b) can be written in discrete form as

$$I'_n = \sum_m B_{nm} I_m \qquad (4)$$

where I'_n is the computed (sampled) spectrum, I_m is the sampled interferogram, and B_{nm} is the transform matrix derived from the continuous transform (2b). Each sampled value of the computed spectrum is a sum of products between successive samples of the interferogram and the coefficients in the corresponding row of B_{nm}. Thus, all sampled values I'_n can be computed simultaneously by the data acquisition array processor whose diagram is shown in Fig.4. Each processing channel of the array processor corresponds to one sampled value of the spectrum. The incoming interferogram is converted into a data stream by a free-running analog-to-digital converter (ADC - TDC1007, TRW), and the data are broadcast on the "Data In" bus. The ADC is strobed by a clock, which is phase locked to the photoelastic modulator driver, and which multiplies the driving frequency, ω_0, by a number that determines the number of interferogram samples per modulator period (typically 100-fold frequency multiplication, for a strobe frequency 8.5 MHz). The same strobe signal drives a counter (address generator) that indexes the interferogram samples. The counter is reset by the phase reference signal, and thus the sample index returns to zero during each period of the modulator. The indices are broadcast on the "Index" bus.

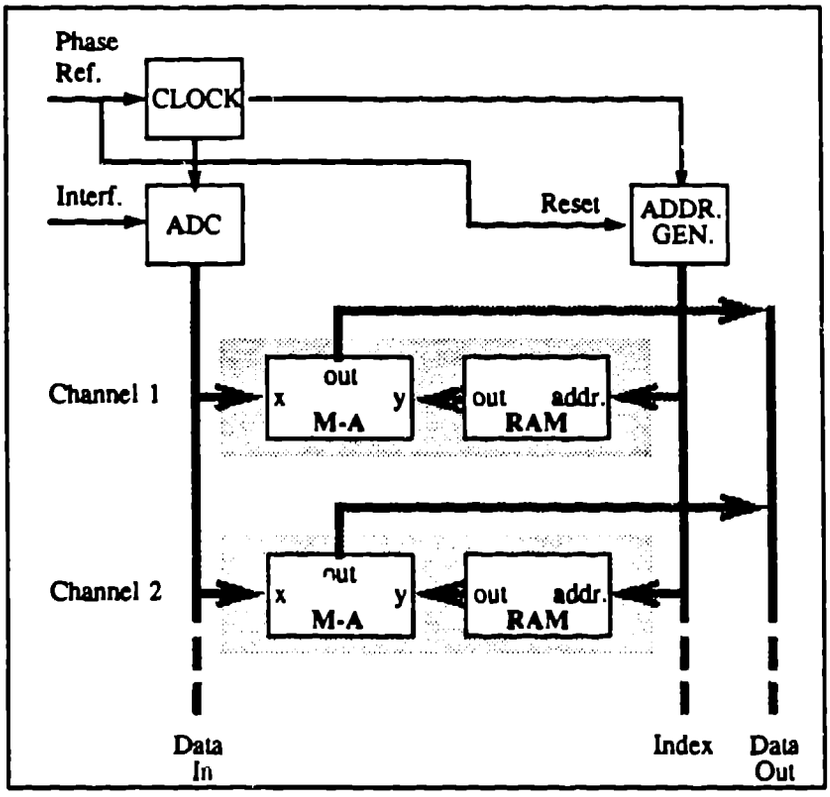

Figure 4. Block diagram of the data acquisition array processor, showing two signal processing channels. ADC-analog-to-digital converter; M-A - multiplier-adder; RAM - random access memory.

Each processing channel consists of a multiplier-adder (TDC1008, TRW) and random access memory (RAM). The coefficients for each sampled value of the computed spectrum (the corresponding row of B_{nm}) are stored in RAM. Each channel of the array processor receives a sequence of sampled values of the interferogram and the corresponding sample indices. The index is used to address the RAM, which presents a coefficient B_{nm} to one input of the multiplier-adder, while the other input receives the corresponding interferogram sample. For each period of the clock, the interferogram sample is multiplied by a transform coefficient, and the product is added to an internal register. Thus, each channel computes one sampled value, I'_n, as the interferogram is being acquired. It should be pointed out that the transform matrix, B_{nm}, which is programmed into the array processor memory, is not limited to the discrete version of the transform kernel in (2b). As discussed in Section 4, other transform matrices may be used for the real-time computation of different sets of spectral parameters.

The array processor is controlled by a host computer (not shown in Fig. 4), which downloads the transform coefficients to the processor channels and reads, over the "Data Out" bus, the computed values of the spectrum. The results of the computations can also be read from the "Data Out" bus by other devices, such as data-storage and sort-control devices in flow cytometers and frame buffers in imaging instruments. This local data transfer can take place without the intervention of the host computer, thus ensuring a very high data throughput.

4. MODES OF ANALYSIS

We have already described the spectral analysis mode, in which the array processor channels compute, in parallel, a discretely sampled light spectrum. In this mode, the processor channels are programmed to have adjacent bandpass spectral characteristics. This mode of analysis is illustrated in Fig.5, where interferograms and the corresponding spectra are shown for monochromatic light and for the fluorescence of cells stained with propidium iodide. However, in most biological applications, it is not the fluorescence spectrum that is of interest, but rather the contributions of a given set of fluorochromes to the total fluorescence [8]. Given a set of N simultaneous fluorochromes with normalized, sampled emission spectra, $s_n = (s_{mn})$, and with emission intensities α_n, the total fluorescence spectrum, $s = (s_m)$, is

$$s_m = \sum_{n=1}^{N} s_{mn}\alpha_n \quad m = 1,\ldots,M \qquad (5a)$$

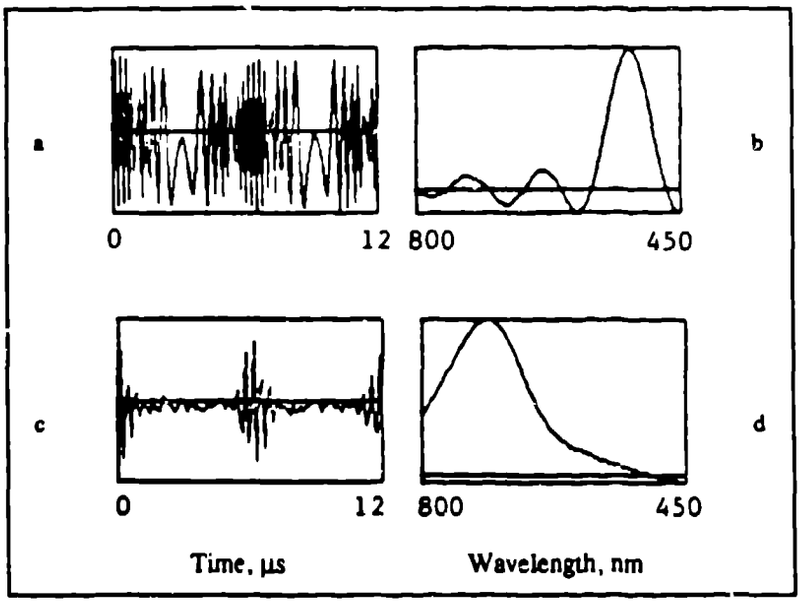

Figure 5. Interferograms and computed spectra for 488 nm monochromatic light (a, b) and for the fluorescence of cells stained with propidium iodide (c, d).

where M is the number of sampled values of the spectra. Equation (5a) can be rewritten in vector form as

$$s = S\alpha \qquad (5b)$$

where s and α are the column vectors representing the total spectrum and the individual fluorochrome intensities, and S is the M by N matrix containing the fluorochrome spectra as its columns. Because, in general, the fluorochrome spectra, S, are known, and the total emission spectrum, s, can be determined by the FT spectrometer, the individual fluorochrome intensities, α, can be obtained by solving Eq. (5b). The solution can be shown to be

$$\alpha = S's \qquad (5c)$$

where $S' = (S^TS)^{-1}S^T$, with S^T being the transposed of the matrix S. The same problem can be similarly formulated in the interferogram, rather than the spectrum, domain. In the interferogram domain, the equations equivalent to Eqs. (5b, 5c) are

$$w = W\alpha \qquad (6a)$$

$$\alpha = W'w \qquad (6b)$$

where w is the interferogram for the total fluorescence, W is the matrix containing the normalized interferograms for the individual fluorochromes as its columns, and $W' = (W^TW)^{-1}W^T$. The matrix, W, is M by N, where M is the number of sampled values of the interferogram. As the spectrum and interferogram are related by $s = Bw$ [from Eq. (4)], the matrices S and W are related by $S = BW$. Thus, one can easily move between the interferogram and spectrum domains.

In practical terms, the base spectra used for resolving the total fluorescence can be acquired by the spectrometer or can be read from a data base, following which the host computer forms the spectral matrix, S, and computes its interferogram domain equivalent, W. Alternatively, the instrument can acquire base interferograms (for example, interferograms for individual fluorochromes) and form the matrix W directly. The host computer then computes the matrix W', following which the N rows of W' are stored in N channels of the array processor. This ensures that, during the acquisition of the interferogram, each channel will compute one coefficient α_n. Such a mode of analysis is illustrated in Fig.6. The emission spectra of polystyrene microspheres stained with either fluorescein or propidium iodide were acquired by the FT flow cytometer. The two emission spectra are shown in Fig. 6a, together with the optimal spectral characteristics computed by the host computer. These spectral characteristics are shown both in the spectrum and the in-

terferogram domain, the latter form being the one that is downloaded to the array processor for real-time processing. Figure 6b shows a scattergram of the outputs of the two processing channels, programmed with the spectral characteristics in Fig. 6a, for a mixture of the two types of microspheres. One can clearly see the separation of the events according to their spectral properties.

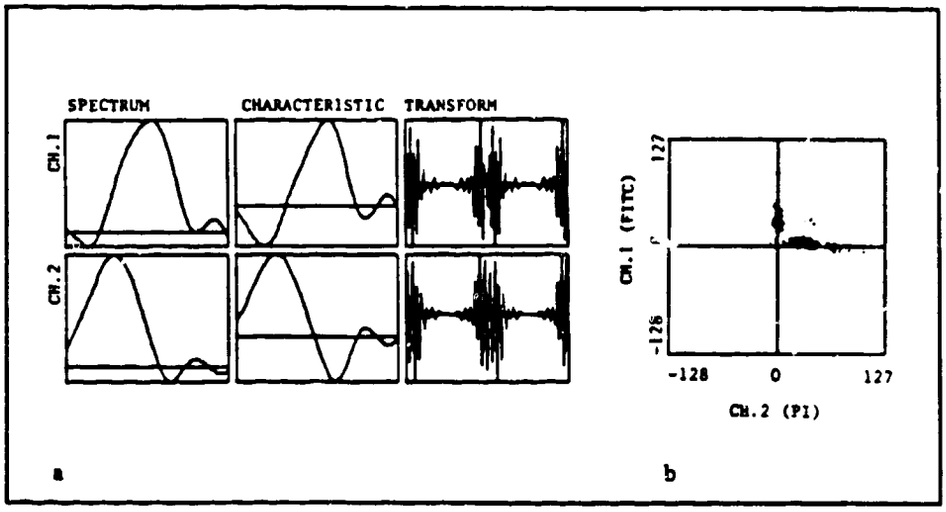

Figure 6. Separation of contributions from fluorescein and propidium iodide: fluorochrome spectra and optimum spectral characteristics (a), and scattergram for a mixture of microspheres stained with the two fluorochromes (b). FITC-fluorescein; PI-propidium iodide.

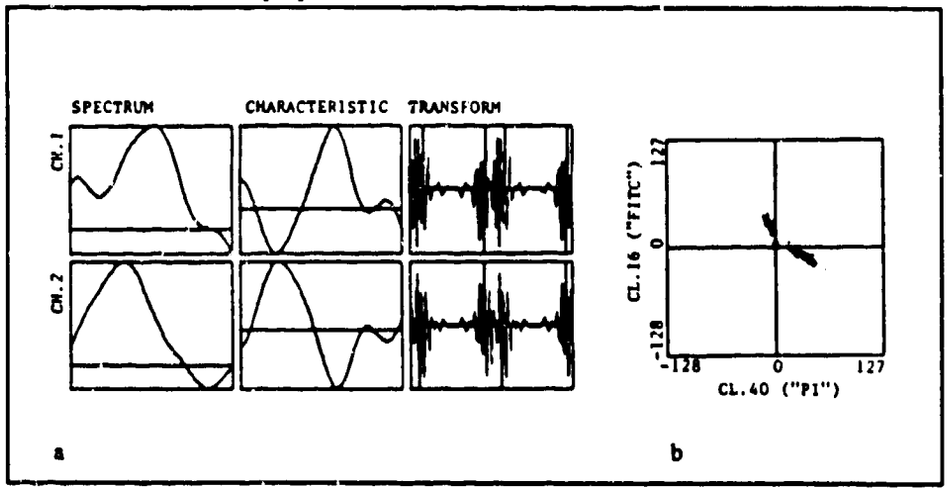

Figure 7. Analysis in terms of mean spectra of spectral clusters: mean spectra and optimum spectral characteristics (a), and scattergram for the same microsphere mixture used in the cluster analysis (b).

The base spectra can also be chosen to be the mean spectra of cell or pixel subpopulations, in which case the computed spectral parameters provide a measure of the similarity of each particle or pixel to the "base" subpopulations. When using this mode of analysis, the instrument may not require a priori information about the specimen, as a statistical analysis performed by the host computer on a set of spectra acquired by the instrument may reveal the existence of spectrally distinct subpopulations (clusters). Following the cluster analysis, the mean spectra of the subpopulations can be computed and subsequently used as base spectra. This is an "adaptive" mode of operation, in which the instrument programs itself automatically to enhance the differences in the spectral properties of the subpopulations in a given sample. Such a mode of analysis is illustrated in Fig.7. The same fluorescein and propidium iodide stained microspheres were used in this experiment. However, instead of analyzing each type of microsphere to obtain fluorochrome base spectra, the instrument analyzed a mixture of microsphere and then performed a cluster analysis on the spectra of 100 particles. The mean spectra of the two largest clusters were taken as base spectra (Fig. 7a), and the array processor was programmed accordingly. The scattergram in Fig. 7b was obtained by analyzing the same mixture of microspheres. It can be clearly seen that the two spectrally distinct types of microspheres appeared indeed as well separated clusters in the scattergram.

Finally, the base spectra (or interferograms) used in the spectral analysis of fluorescence need not be the emission spectra of individual fluorochromes. For example, when using metachromatic fluorochromes, one can use a set of characteristic emission spectra for each such fluorochrome as base spectra [9]. Consequently, the spectral parameters computed by the array processor will provide a "meaningful" description of the state of the metachromatic fluorochromes in each cell or in each pixel, while also possibly reducing the amount of spectral data to be stored and analyzed.

5. SPECTRAL FLUORESCENCE IMAGING

The real-time FT spectrometer can be used both in flow cytometers and imaging systems. Although the large useful apertures of photoelastic modulators allow them to be used in conventional imaging systems, such an approach to spectral imaging requires a fast response, position-sensitive detector, such as an image dissector. Furthermore, the phase difference introduced by the interferometer would depend on the direction of the light rays passing through the modulator, and, thus, the coefficients of the transform would depend on the position of the pixel being analyzed. A more practical approach is to incorporate the spectrometer into a laser-scanned fluorescence imaging system, where a photomultiplier can be used for detection, and where light rays follow the same path through the modulator, regardless of the position of the sample volume being analyzed. A block diagram of an imaging system incorporating a real-time FT spectrometer is shown in Fig. 8, which also includes, for comparison purposes, the block diagram of the corresponding flow instrument (Fig. 8a). One can see that the interferometer, including the detector, replaces the photomultiplier normally present in a laser-scan microscope. From the point of view of the electronics, the only differences between the flow and imaging systems are the following: (i) the data-storage and sort-control electronics that receive the output of the array processor in the flow system are now replaced by a bank of frame buffers, each of them connected to the output of a processing channel; and (ii) the control logic ("CLOCK" in Fig.8) controls the scanner driver circuits. The image acquisition and processing system described in Fig. 8 can generate concurrently multiple images, each enhanced for a particular emission spectrum. The spectral analysis time for each pixel remains, as in the case of the flow system, independent of the number of spectral parameters and, therefore, of the number of enhanced images that are being processed. This analysis time has, for the actual system described in this article, a minimum value of less than 3.2 μs.

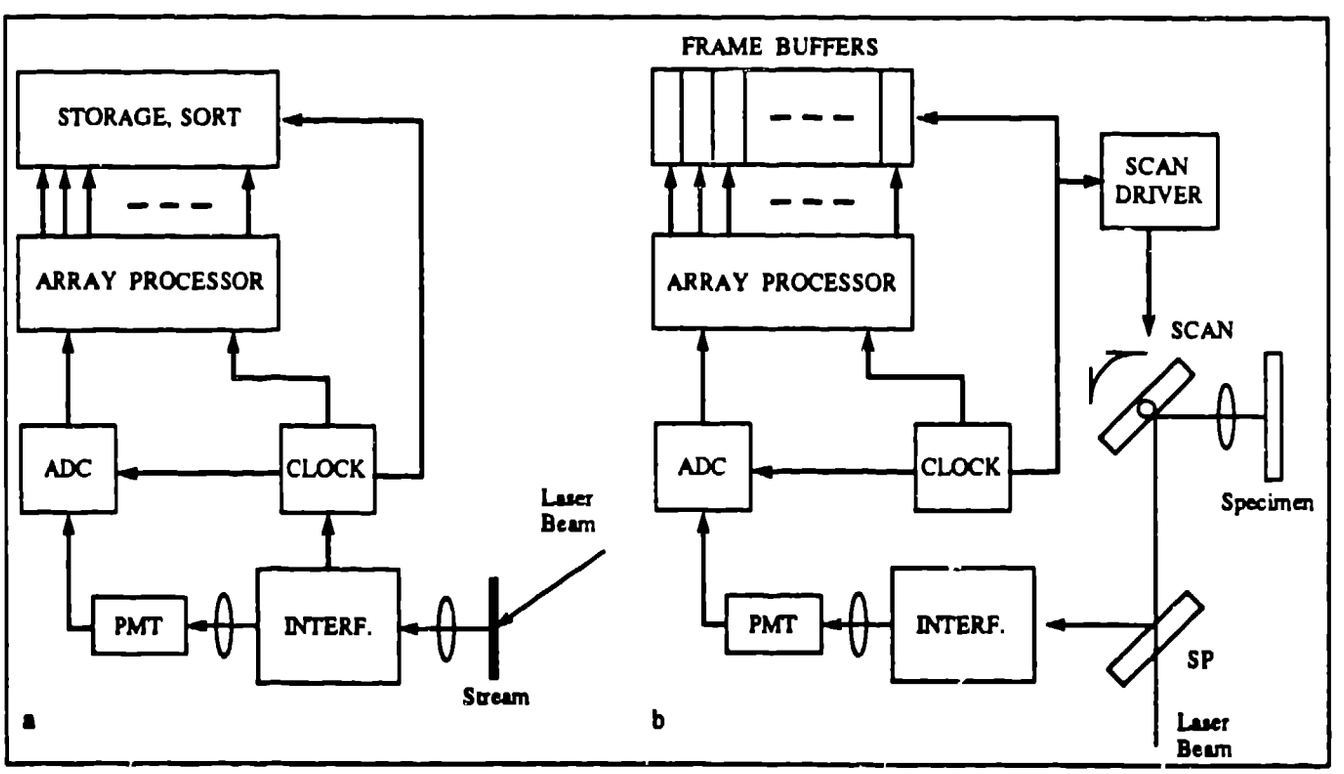

Figure 8. Use of the real-time FT spectrometer in flow cytometry (a) and fluorescence imaging (b). ADC-analog-to-digital converter; PMT-photomultiplier; SP-short-pass dichroic mirror; INTERF-birefringent interferometer.

In addition to the modes of analysis described in the previous section, one can envisage a mode that is specific to imaging applications and which takes advantage of the morphological information that may be present in images that have not been spectrally enhanced. Thus, if a morphologically interesting structure has been detected either by an image processing system or by the operator, the average spectrum of that structure can be used as a base spectrum, and an image enhanced for that particular spectrum can be generated. The spectrally enhanced image may reveal other similar morphological structures that were not apparent in the original image, or it may also reveal structures that are spectrally, but not morphologically, related.

6. THE INTEGRATION OF FLUORESCENCE ANALYSIS BY FLOW AND IMAGING

The instruments shown in Fig. 8 share not only the spectrometer optics and electronics, but also the basic modes of analysis and the format of the data (base spectra) used to program them. If a communication channel is established between the two instruments (for example, by having the same CPU control both instruments, or by having multiple CPUs on the same backplane), then these instruments can cooperate in the following ways: (i) base spectra for resolving total cell/pixel fluorescence can be shared; and (ii) the spectral data obtained by one instrument can be used to program the other. Indeed, if the analysis of a cell suspension reveals the existence of a spectrally distinct subpopulation, then the average spectrum for that population can be transferred to the spectral imaging microscope, where it can be used to enhance the image of whole cells or morphological details that have the same spectral properties. Conversely, the average spectrum of a whole cell of interest, or that of a particular morphological detail, can be transferred to the flow instrument, where it can be used to identify and quantitate cell subpopulations with the same spectral properties.

The integration of flow and imaging at the level of the spectral analysis parameters creates a direct connection between population data and high-resolution morphological information at the level of the single cell. Such a connection simplifies the interpretation of multiparameter population data in a manner that is similar to the sorting of subpopulations, followed by microscopic observation. This "virtual sorting" of cells only requires the recovery and analysis of data, while providing the same correlated information normally provided by physical sorting. The converse process, which could be called "reversed virtual sorting" and which has no equivalent in conventional flow and imaging analysis, allows morphologically distinct cell types to be rapidly identified and quantitated in large cell samples.

7. CONCLUSIONS

The birefringent modulator, in conjunction with a real-time, parallel signal processor, can be used successfully as the basis of a fast FT spectrometer that is suitable for flow cytometry applications. With simple modifications, the same device can be used for single pixel spectral analysis in a laser-scan fluorescence microscope.

The FT spectrometer described in this article combines high-speed spectral analysis with a high degree of flexibility in the choice of spectral parameters. Furthermore, redefining the spectral parameters is no longer an operation that involves choosing and replacing optical filters, but, like other aspects of the operation of the instrument, is a purely numerical operation that can be completely automated. Further automation is possible in an integrated flow and imaging system, where direct and reversed virtual sorting allow data obtained by one type of instrument to be used directly in the interpretation of the data obtained by the other.

8. ACKNOWLEDGMENTS

This work was supported in part by LANL through ISRD award X91P and by the National Flow Cytometry Resource.

9. BIBLIOGRAPHY

[1] Wade, C.G., R.H. Rhyne, W.H. Woodruff, D.P. Bloch and J.C. Bartholomew, "Spectra of Cells in Flow Cytometry Using a Vidicon Detector.", J. Histochem. Cytochem. 27, 1049 (1979).

[2] Steen, H.B. and T. Stokke, "Fluorescence Spectra of Cells Stained With a DNA-Specific Dye, Measured by Flow Cytometry", Cytometry 7, 104 (1986).

[3] Bell, R.J., "Introductory Fourier Transform Spectroscopy", Academic Press, New York (1972).

[4] Griffiths, P.R. (ed.), "Transform Techniques in Chemistry", Plenum Press, New York (1978).

[5] Buican, T.N., "Fourier Transform Flow Cytometry - The Interferometric Analysis of Emission Spectra from Individual Cells", Abstract 502, XI Int. Conf. Analytical Cytology, Hilton Head, SC (1985).

[6] Buican, T.N., "An Interferometer for Spectral Analysis in Flow", Abstract 734, XII Int. Conf. Analytical Cytology, Cambridge, England (1987).

[7] Buican, T.N., "A Multiple Bus Data Acquisition, Processing, and Control System for Flow Cytometry", Abstract 737, XII Int. Conf. Analytical Cytology, Cambridge, England (1987).

[8] Buican, T.N., "Spectral Analysis in Flow: The Fourier Transform Flow Cytometer", *In* "Clinical Cytometry and Histometry" (G. Burger, J.S. Ploem and K. Goerttler, eds), p. 66, Academic Press, London (1987).

[9] Cooper, J., T. Buican, H. Crissman and W. Wharton, "Fourier Transform Flow Cytometric Analysis of Cells Labelled With a Metachromatic Dye", Abstract 493, XII Int. Conf. Analytical Cytology, Cambridge, England (1987).